

## Simulated interannual to decadal variability in the tropical and sub-tropical North Atlantic

Thomas L. Delworth

Geophysical Fluid Dynamics Laboratory/NOAA, Princeton, New Jersey 08542

Vikram M. Mehta

NASA-University of Maryland Joint Center for Earth System Science, Department of Meteorology, University of Maryland, College Park, Maryland 20742

**Abstract.** The dominant pattern of tropical and sub-tropical North Atlantic sea surface temperature (SST) anomalies simulated in the GFDL coupled ocean-atmosphere model is identified and compared to observations. The spatial pattern and temporal variability of that pattern resemble observational results. On interannual time scales it is shown that anomalous surface heat fluxes, consistent with variations in the intensity of the sub-tropical high pressure system in the atmosphere and the associated Northeasterly Trade winds, appear to be the most important process for generating this SST pattern. This relationship is also true on decadal time scales, although the relative role of oceanic heat advection is somewhat larger than on the interannual time scales.

### 1. Introduction

Sea surface temperature (SST) variations in the tropical Atlantic influence climate over the neighboring continents at interannual to decadal time scales [see *Mehta* (1998) and references therein]. Decadal scale SST and associated climate variations also have the potential to interact with anthropogenic climate change. Therefore, it is important to understand the physics of these SST variations and assess their predictability.

Over the last decade, analyses [see, for example, *Houghton and Tourre*, 1992; *Mehta and Delworth*, 1995; *Enfield and Mayer*, 1997; *Mehta*, 1998] have shown that *interannual* SST variations in the tropical Atlantic are approximately independent on the two sides of the Equator. Recent analyses [*Mehta*, 1998; hereafter referred to as M98] have also shown that *decadal* scale SST anomalies in the tropical Atlantic are largely independent on the two sides of the Equator. Further, the decadal SST anomalies rotate anticyclonically around each basin (North and South Atlantic) in the sub-tropical ocean gyres, occasionally expanding across the Equator. Various spectrum analyses of these long SST time series do not always show statistically significant spectral peaks at decadal time scales in the North Atlantic. In apparent contrast, decadal spectral peaks are much stronger in the tropical South Atlantic.

In order to assess whether numerical models simulated such variability, *Mehta and Delworth* [1995] (hereafter referred to as MD) compared the then-available observations of decadal

SST variations in the tropical Atlantic with SST variations in a 200 years long climate simulation with the global coupled ocean-atmosphere model developed at the Geophysical Fluid Dynamics Laboratory (GFDL). It was shown in MD that the model-generated decadal SST variations in the tropical Atlantic resemble the observed decadal SST variations. Further, this preliminary analysis also showed that there is little coherence between model-generated decadal SST variations on the two sides of the Equator.

The purpose of the present work is (a) to further clarify characteristics of the model-generated decadal SST variations in the tropical and sub-tropical North Atlantic in light of the more recent analyses of observations and (b) to analyze the physics of these model-generated decadal variations. We ask the following questions: (1) Do the decadal SST anomalies in the model show characteristics similar to the observed decadal SST anomalies? (2) What is the relationship among simulated anomalies in SSTs, sub-surface ocean temperatures, sea level pressure, near-surface winds, and ocean-atmosphere heat fluxes? (3) Which physical processes appear to be most important for generation of the decadal SST anomalies?

### 2. Description of Model and Numerical Experiments

The coupled ocean-atmosphere model used in this study is identical to that described in detail by *Manabe et al.* [1991]. The model is global in domain, with realistic geography consistent with resolution. The model is forced with a seasonal cycle of insolation at the top of the atmosphere. The atmospheric component numerically integrates the primitive equations of motion using a semi-spectral technique in which the variables are represented by a set of spherical harmonics and by corresponding grid points with a typical spacing of 7.5° longitude and 4.5° latitude. There are nine unevenly spaced levels in the vertical. The oceanic component of the model uses a finite difference technique with twelve unevenly spaced levels in the vertical, and a horizontal resolution of approximately 3.7° longitude and 4.5° latitude. The model atmosphere and ocean interact through fluxes of heat, water, and momentum at the air-sea interface.

In order to reduce climate drift, adjustments to the model-calculated heat and water fluxes are applied at the air-sea interface. These flux adjustments are derived from preliminary integrations of the separate atmospheric and oceanic components [see *Manabe et al.*, 1991, for details].

After preliminary integrations to achieve an initial condition in approximate equilibrium, the model was integrated for

a period of 1000 years. The output from this integration forms the main dataset for the analyses presented below.

### 3. Characteristics of Model Variability

Previous analyses (MD) of model SST variations in the tropical and sub-tropical Atlantic revealed a pattern of variability which resembled the dominant empirical pattern of observed SST variability. In the current work an empirical orthogonal function (EOF) analysis was conducted using annual mean model SST from the Equator to 72°N (all model analyses shown are performed on annual mean data). The first EOF is shown in Fig. 1a. This spatial pattern resembles the second EOF (not shown) of observed SSTs, particularly over the tropical and sub-tropical North Atlantic (the EOFs of observed SST were computed using the data and techniques described in M98). This pattern is characterized by an approximately zonal band of SST anomalies spanning the longitudinal extent of the basin from 10°N-25°N. The temporal variability of this pattern of SST variability is characterized by the spectrum of the associated EOF time series. This spectrum, shown in Figure 1b, is generally "red" (i.e., greater vari-

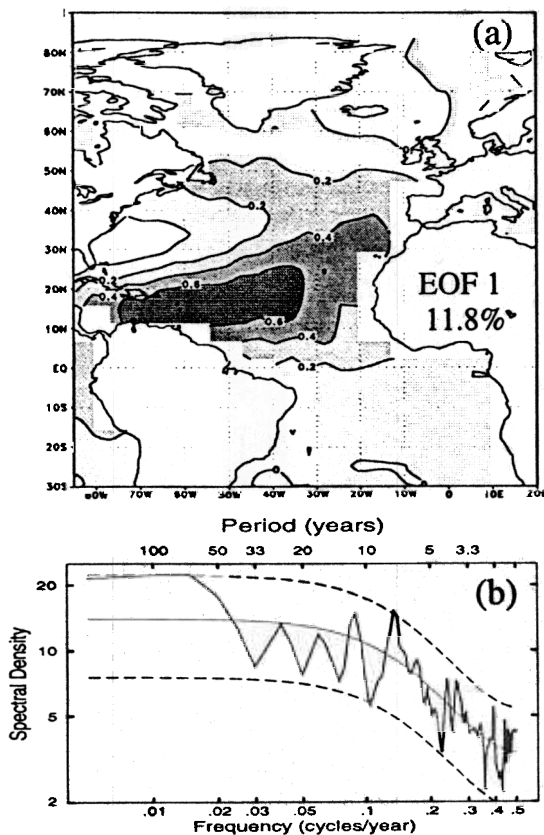


**Figure 1.** (a) First EOF of annual mean model SST over the Atlantic from the Equator to 72°N. The contoured values are the correlation coefficients at each grid point between the EOF time series and the original SST time series at that point. This pattern explains 11.8% of the spatially integrated variance. (b) Fourier spectrum of the corresponding EOF time series. The smooth solid line represents a background "red noise" (first order Markov process) spectrum, while the dashed lines represent an estimate of the 95% confidence limits. The period is listed along the top in years.

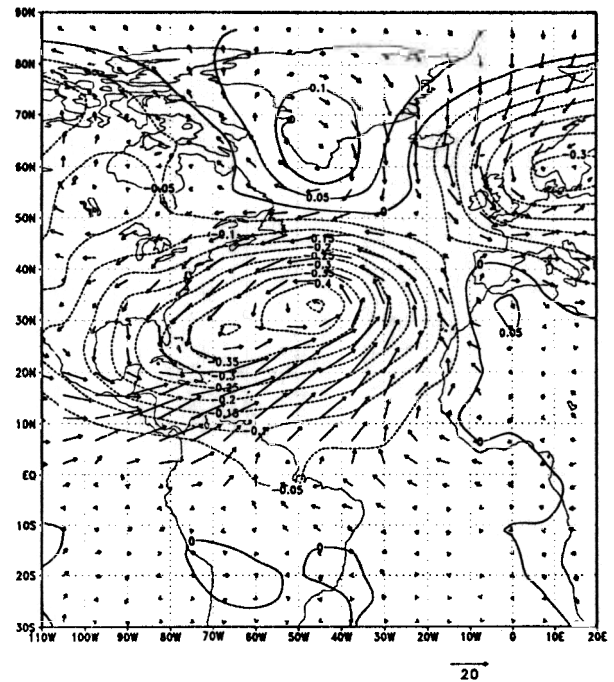


**Figure 2.** Linear regression coefficients of sea level pressure (contours) and near-surface winds (vectors) versus the time series corresponding to EOF 1. For the near-surface winds, each component was regressed against the time series of EOF 1 separately; the results are plotted in vector form, such that the zonal (meridional) component of the vector denotes the magnitude of the zonal (meridional) regression coefficient. The regression coefficients are multiplied by one standard deviation of the EOF time series, so that the fields may be interpreted as the changes corresponding to a one standard deviation increase in the EOF time series; this translates to a maximum SST anomaly of 0.19 °C (the maximum SST value in EOF 1 times one standard deviation of the EOF time series). The units for SLP are mb, and the units for winds are  $\text{cm s}^{-1}$ . The vector at the bottom of the image denotes a wind speed anomaly of  $20 \text{ cm s}^{-1}$ .

ance at low frequencies than at high frequencies), with weak peaks in the decadal range. These peaks do not substantially exceed an estimate of the 95% confidence limits.

The relationship between this pattern of SST variability and other oceanic-atmospheric quantities can be ascertained by computing linear regressions of the form  $y = ax + b$ , where the independent variable ( $x$ ) is the SST EOF 1 time series, and the dependent variable ( $y$ ) is some other oceanic-atmospheric quantity. We compute "a" (slope of the regression line; we refer to this as the regression) to denote the change in "y" for a unit change in "x". Shown in Figure 2 are regressions between sea level pressure (SLP) and the EOF time series (shown by the contours) as well as between atmospheric near-surface winds and the EOF time series (indicated by the vectors). The pattern of SLP variability is characterized by a surface low pressure center to the north of the maximum SST anomalies, suggesting that the atmosphere plays a substantial role in this pattern of oceanic variability. The associated near-surface wind anomalies indicate a reduction in the Northeasterly Trade Winds over the region of positive SST anomalies, which can reduce the latent heat flux from the ocean to the at-

mosphere and warm the near-surface layer of the ocean. The spectrum (not shown) of the temporal fluctuations of this pattern of near-surface wind anomalies resembles "white noise", thus indicating no preferred time scale.

#### 4. Ocean Heat Budget Analysis

In order to quantify the relative contributions of various processes in generating this pattern of SST variability, linear regressions were computed between the terms in the upper ocean heat budget equation and the time rate of change of the EOF 1 time series. Noting that the time series of SST at an individual grid point can be expressed as

$$\sum_{i=1}^M (\text{EOFTS}_i)(\text{EOF}_i),$$

where  $\text{EOFTS}_i$  is the time series for EOF "i", "M" is the number of grid points, and  $(\text{EOF}_i)$  is the eigenvector value for EOF "i" at an individual grid point, the heat budget of the uppermost model oceanic layer can be expressed as,

$$C \sum_{i=1}^M \frac{\partial}{\partial t} (\text{EOFTS}_i)(\text{EOF}_i) = -C \vec{v} \cdot \vec{\nabla} T - LH - SH + R + \text{Conv}t - \text{Diffusion} + \text{Adjustment} \quad (1)$$

The heat capacity of the layer is given by  $C$  (=mass of the layer times the specific heat),  $\vec{v}$  is the three dimensional velocity,  $\vec{\nabla} T$  is the three dimensional gradient of temperature,  $LH$  and  $SH$  are the latent and sensible heat fluxes from the ocean to the atmosphere,  $R$  is the net radiative forcing at the surface, "Conv $t$ " is the equivalent heat flux corresponding to the temperature change due to oceanic convection, "Diffusion" is the equivalent heat flux corresponding to the sum of horizontal and vertical diffusion, and "Adjustment" represents the heating due to the flux adjustments. All terms can be expressed in  $\text{W m}^{-2}$  for a 50.9 m. layer (the thickness of the uppermost layer of the ocean model), and were estimated from monthly mean model output. The flux adjustments are precisely the same from one year to the next, so that there are no interannual anomalies of the flux adjustment term.

The contribution of the various terms in (1) to the generation of the spatial pattern in Figure 1a is estimated by computing regressions of the heat budget terms versus the temporal derivative of the time series of EOF 1. There is a clear similarity between the spatial pattern (not shown) of the heat flux variations (the sum of the sensible, latent, and radiative components) and the pattern of SST anomalies shown in Figure 1a, suggesting that anomalous surface heat flux variations help to drive the pattern in Figure 1a. The weakening of the Northeasterly Trade Winds (indicated in Figure 2) reduces the latent heat flux from the upper ocean layer to the atmosphere, thereby warming that ocean layer. Analyses of the individual terms (not shown) of the surface heat flux reveal that the latent heat flux variations are the most important for this pattern of variability. The largest SST anomalies occur in the same locations as the largest surface heat flux anomalies.

Regressions of the heat advection (not shown) also resemble the SST pattern in Figure 1a, but the magnitudes of the regression coefficients are generally smaller than the surface heat flux terms. Physically, the weakening of the atmospheric sub-tropical high pressure system and associated reductions in the surface pressure gradient alter the atmosphere to ocean momentum flux and weaken the oceanic sub-tropical gyre.

This, in turn, reduces the southward advection of relatively cold water in the eastern portion and the northward advection of relatively warm water in the western portion of the sub-tropical North Atlantic. This leads to a warming off the west coast of Africa and a cooling off the east coast of the U.S. The anomalous atmospheric circulation also reduces the upwelling of colder, sub-surface water off the coast of Africa, further warming the near-surface water in that region.

In order to explicitly examine decadal SST variations, the above set of analyses were repeated after filtering the SST and heat budget terms with a 5 to 30 year band pass filter. The first EOF of SST (not shown) strongly resembled the results from the unfiltered analyses. The regressions for the air-sea heat fluxes and the heat advection are shown in Figure 3. For the filtered data, the relative contribution of the advective terms is somewhat larger than for the unfiltered data, suggesting that oceanic advective processes in this model are more important for this pattern of variability on the decadal time scale than on the interannual (unfiltered) time scale. However, even on the

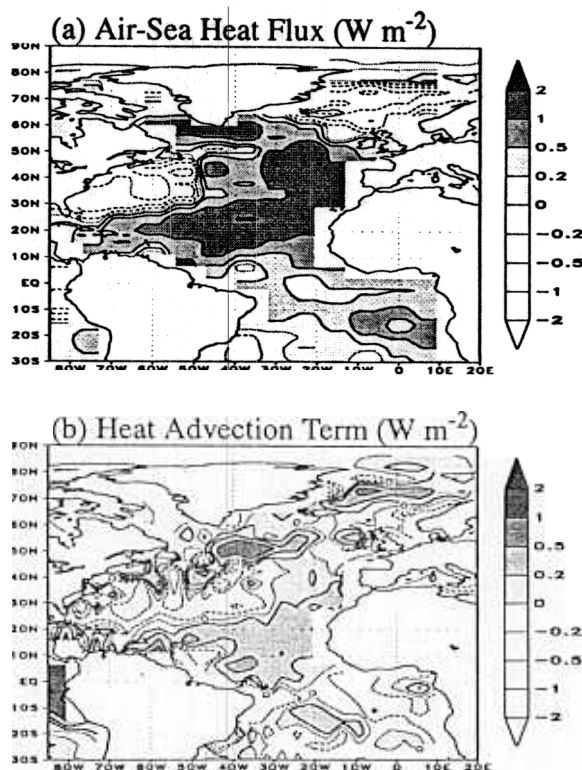


Figure 3. (a) Map of the regressions between the time series of the air-sea heat flux and the temporal derivative of the time series of EOF 1 (of the 5-30 year filtered data). Positive values denote a flux which would tend to warm the uppermost ocean layer. Prior to the regression analysis, all quantities were filtered such that only time scales between approximately 5 and 30 years were retained. Units are  $\text{W m}^{-2}$ . The regression coefficients are multiplied by one standard deviation of the EOF time series (1.27), so that the fields may be interpreted as the changes corresponding to a one standard deviation increase in the EOF time series; this translates to a maximum SST anomaly of  $0.18^\circ\text{C}$  (the maximum SST value in EOF 1 times one standard deviation of the EOF time series). (b) Same as (a) but using the total oceanic heat advection (horizontal and vertical) instead of the air-sea heat flux.

decadal scale the ocean-atmosphere heat flux term was still substantially larger than the advective term.

The above results suggest that *for this model and this pattern of SST variability*, the relative contribution of the advective terms is smaller than that of the ocean-atmosphere heat flux. It must be noted, however, that in this model the simulated oceanic currents are substantially weaker than the observed currents. Thus, it is certainly possible that in a model with stronger oceanic currents the relative role of the oceanic heat advection terms could be substantially larger than suggested by the present model results. Efforts to explore this issue are currently underway with a higher resolution coupled model.

The above results were strengthened by examining the output from an additional experiment in which the same atmospheric model was coupled to a 50 m. deep "slab" ocean. This simple ocean model interacts with the atmosphere through exchanges of sensible, latent, and radiative heat fluxes. In addition, a seasonal cycle of heat flux convergence is prescribed at each grid point to mimic the effects of oceanic heat transports which are not represented in the "slab" model; this helps to create a seasonal cycle of SSTs in the "slab" model which is similar to that in the fully coupled model. A 500 year integration was performed with this model, and the output was analyzed. The pattern of SST variability shown in Figure 1a is also present in this model (not shown; the pattern appears as the second EOF), confirming that this pattern of variability can be generated through variations in air-sea heat fluxes without interannual variations in oceanic heat advection.

Since the observed decadal SST anomalies were found to rotate anticyclonically around the North Atlantic [Hansen and Bezdek, 1996; Sutton and Allen, 1997; M98], complex EOF analysis was applied to the fully coupled model SSTs. The results (not shown) show a small tendency for SST anomalies to propagate anticyclonically around the sub-tropical gyre in the North Atlantic. In order to further explore this, complex EOF analysis was also conducted on ocean temperatures at model level 2 (a depth of 85 m.). The results (not shown) indicate sub-surface temperature anomalies rotating around the sub-tropical gyre. It remains an open question why the rotation of simulated ocean temperature anomalies is so evident in the sub-surface layer but not at the surface, and whether these rotating anomalies feed back to the atmosphere.

## 5. Discussion

We have focused our analyses on the characteristics of simulated SST variability in the tropical and sub-tropical North Atlantic. The model simulated variability resembles observed variability in both spatial pattern and temporal behaviour.

The model results suggest that variations of the surface heat and momentum fluxes are capable of forcing this pattern of variability. The associated atmospheric variability has a large-scale spatial structure (Figure 2) but does not have a distinct timescale. It is tempting to speculate that this pattern of SST variability can thus be *partially* regarded as an oceanic response to surface heat and momentum flux variations associated with atmospheric variability. The rotation of sub-surface ocean temperature anomalies around the sub-tropical gyre may be excited by this pattern of atmospheric variability.

While additional physical processes contribute to the generation of tropical and sub-tropical North Atlantic SST variability in the real climate system, it is likely that the primary

physical mechanism identified in this modeling study (latent heat flux forcing) plays a large role in the real climate system. The results of a recent ocean modeling study support this [Carton, 1996], as do recent analyses of observational data [Enfield and Mayer, 1997]. The results of Chang [1997] also stress the important role of anomalous heat fluxes.

A number of questions remain regarding tropical Atlantic variability in general and these model results in particular. (1) Is the pattern of SST variability discussed here part of a coupled air-sea mode involving two-way interactions? (2) Is there a discernible decadal time scale in tropical North Atlantic SSTs? Both model and observational results suggest a weak decadal peak which does not stand out against background noise if commonly employed statistical techniques are used. Analyses of this and other coupled ocean-atmosphere models are in progress to address these questions.

**Acknowledgments.** The authors would like to thank R.J. Stouffer and S. Manabe for use of their model output. Comments of Drs. P. Chang, I. Held, S. Klein, and B. Soden on an earlier version of this manuscript are gratefully appreciated. VM was partially supported by NASA-Physical Oceanography grant 6224745.

## References

- Chang, P., L. Ji, and H. Li, A decadal climate variation in the tropical Atlantic Ocean from thermodynamic air-sea interactions, *Nature*, 385, 516-518, 1997.
- Carton, J.A., X.Cao, B.S. Giese, and A.M. daSilva, Decadal and interannual SST variability in the Tropical Atlantic Ocean, *J. Phys. Oceanogr.*, 26, 1165-1175, 1996.
- Enfield, D.B., and D.A. Mayer, Tropical Atlantic sea surface temperature variability and its relationship to El Nino-Southern Oscillation, *J. Geophys. Res.*, 102, 929-945, 1997.
- Hansen, D.V., and H.F. Bezdek, On the nature of decadal anomalies in North Atlantic sea surface temperature, *J. Geophys. Res.*, 101, 8749-8758, 1996.
- Houghton, R.W., and Y.M. Tourre, Characteristics of low-frequency sea surface temperature fluctuations in the Tropical Atlantic, *J. Climate*, 7, 765-771, 1992.
- Manabe, S., R.J. Stouffer, M.J. Spelman, and K. Bryan, Transient response of a coupled ocean-atmosphere model to gradual changes of atmospheric CO<sub>2</sub>. Part I: annual mean response, *J. Climate*, 4, 785-818, 1991.
- Mehta, V.M., and T. Delworth, Decadal variability of the tropical Atlantic Ocean surface temperature in shipboard measurements and in a global ocean-atmosphere model, *J. Climate*, 8, 172-190, 1995.
- Mehta, V.M., Variability of the tropical ocean surface temperatures at decadal-multidecadal time scales, Part I: The Atlantic Ocean, *J. Climate*, in press.
- Sutton, R.T., and M.R. Allen, Decadal predictability of North Atlantic sea surface temperature and climate, *Nature*, 388, 563-567, 1997.
- Thomas L. Delworth, Geophysical Fluid Dynamics Laboratory/NOAA, Princeton, NJ 08542 U.S.A. (e-mail: td@gfdl.gov)
- Vikram M. Mehta, NASA-University of Maryland Joint Center for Earth System Science, Department of Meteorology, University of Maryland, College Park, MD, 20742 U.S.A. (e-mail: mehta@atmos.umd.edu)

(Received March 11, 1998; accepted June 11, 1998)